Effect of temperature on ultrasound-assisted electroless nickel-boron plating

V. Vitry*, L. Bonin

Metallurgy Lab, University of Mons, Mons, Belgium

ABSTRACT

Electroless nickel-boron coatings have several advantages over electroplated nickel and electroless nickel-phosphorous: they are harder than both other coatings and, as all electroless coatings, can be applied easily to complex shapes and all substrates, even non conducting ones, contrary to electroplated coatings. Preliminary testing has proved that ultrasound assistance helps improve their properties by increasing the plating rate while conserving the properties of the coating.

In this study, the effect of plating temperature on mechanically agitated and ultrasonic assisted electroless nickel-boron deposition was investigated: deposition was performed in two different configurations: one with a classical mechanical agitation at 300 rpm and the other employing ultrasound at a frequency of 35 kHz. In addition, different temperatures in the 80–95 °C range were tested. The increase of plating rate previously observed was confirmed and it was possible to lower slightly plating temperature while conserving plating efficiency, which decreases evaporation of the solution. Morphological, mechanical, corrosion and wear characterization were performed on the coatings, as well as tribocorrosion studies in an alkaline environment (0.1 M NaCl). Ultrasound-assisted coatings presented tribocorrosion behaviour that was similar or better than the standard ones.

1. Introduction

Electroless nickel plating, while it can be considered as a mature industry, due to its prolonged use since the first application in 1946 [1], has known a lot of improvements and modifications, including the development and use of electroless nickel-boron [2]. Electroless nickel coatings present unique properties- high corrosion resistance, excellent wear resistance, thickness uniformity and shape compliance, magnetic properties, catalytic abilities,… [3–6] – that make them prime candidates for several types of applications in various industries such as electronics, automotive, aerospace, medical, petrochemical, food and military. The most widely used electroless nickel coatings are reduced by sodium (or potassium) hypophosphite and contain a significant amount of phosphorus, they're called nickel-phosphorous (ENP). Electroless nickel-boron (ENB), on the other hand, is obtained by reduction with amine borane compounds or sodium borohydride and different from ENP by their increased hardness (up to 900 hv_{100}) [7–9] and improved wear and scratch resistance. Electroless deposition based on reduction by the borohydride ion has been extensively studied in the last 3 decades and the deposition mechanisms and role of various bath reactive can be found in the literature [10–17].

In comparison to electroplated nickel, electroless coatings present excellent morphological compliance, allowing to plate components with complex shapes and blind holes with homogeneous thickness and can also be used to plate non-conductive substrates.

The use of ultrasound to promote electro and electroless nickel plating has been the object of intense interest in recent years because of the beneficial effect of ultrasound on electrochemical processes [18–23]

and specifically on electroless reduction [24–31]. Studies on nickel deposition have shown that the use of ultrasound improves deposition rate [19,24,25,32] and nucleation [29,33], increase deposit hardness [19,20,23,32], decrease residual stress [20,23], enhance wear resistance and adhesion [20,24] and allow decrease of plating temperature [26,30].

Numerous studies have focused on nickel electroplating and electroless nickel-phosphorus plating (ENP) [20,23,25–28,31] but only a few are dedicated to the effect of ultrasound on electroless nickel-boron coatings: if studies about catalytic powder formation [34,35] and bath using amineborane compounds [36] are excluded, only 2 studies are dedicated to ultrasound assistance in electroless plating [37,38].

In a preliminary study, we successfully used ultrasound to improve the plating rate of ENB from a bath using sodium borohydride [37] and were able to show that the use of a 35 kHz ultrasound bath lead to increased thickness but also smoother surface texture and decreased roughness, without detrimental effects on the hardness, wear or corrosion behaviour of the coating. In this study, the effect of temperature on mechanically agitated and ultrasound assisted electroless nickel-boron plating will be investigated in order to assess the possibility of decreasing plating temperature. A decrease of temperature would allow decreasing evaporation of the plating solution, which leads to loss of energy but also to process control problems. A significant decrease of plating temperature (down to 80 °C) could also open new possibilities for the use of electroless nickel-boron on polymers.

* Corresponding author.

Table 1
Bath composition of sodium borohydride reduced electroless Ni bath.

Nickel chloride	24 g/l
Sodium hydroxide	39 g/l
Ethylenediamine NH_2 CH_2 CH_2 NH_2	60 ml/l
Lead tungstate	0.021 g/l
Sodium borohydride	0.602 g/l

2. Experimental details

2.1. Preparation of substrate

The substrate used for this study was mild steel (St 37), in the shape of sheet coupons with 25 * 50 * 1 mm size. A 2 mm hole was drilled close to one edge for hanging and handling of the samples.

Surface preparation before plating included grinding with SiC paper (180, 500 and 1200 grit successively), then rinsing with deionized water and degreasing with acetone.

The final step, carried out just before the plating process, was activation in 30 vol% HCl for 3 min, followed by rinsing in flowing deionized water and direct immersion in the plating bath.

2.2. Electroless nickel plating

The plating solution (1L per sample, to keep the bath load at 25 cm^2. L^{-1}), was prepared and heated on a temperature-controlled hotplate with mechanical agitation (magnetic stirring). The bath used in this study was developed by Delaunois et al. [39] composition is presented in Table 1. It uses sodium borohydride as reducing agent and lead tungstate as the stabilizer. Operating pH is 12 ± 1. The usual plating temperature with this bath is 95 °C. In this study, relatively lower temperatures (80, 85 and 90 °C) were investigated. Plating time was 1 h for all the tests carried out in this study.

Two plating methods were used in this study, that differ mostly by their agitation means (Fig. 1).

First, magnetic stirring on a hot plate with temperature control was used to represent standard mechanical agitation (Fig. 1a). The rotation speed of the magnetic agitator was maintained at 300 rpm. Second, an ultrasound bath, with a frequency of 35 kHz and a power of 0.065 W/cm (estimated by the calorimetric method [22]) was used for stirring, and an immersion heater was used for temperature control (Fig. 1b).
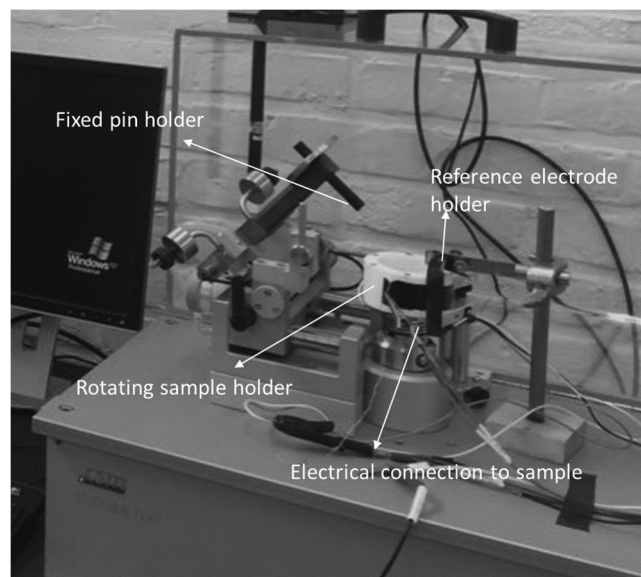

Fig. 2. Tribocorrosion measurement system.

2.3. Coating characterization

Morphology of the coating (in cross-section and on the surface) was observed by both optical microscopy, using a HIROX KH-8700 Digital Optical Microscope, and scanning electron microscopy (SEM) with a Hitachi's SU8200 microscope. The Image J image analysis software was used to evaluate the size of features present on the coating.

Hardness was obtained by Knoop microindentation, with a Mitutoyo HM-200. Measurements were carried out on polished cross-section, with a load of 50 gf and a load exertion time of 20 s. Hardness values are the average of 10 measurements at least, on at least 2 distinct samples.

Roughness measurements were carried out using a Zeiss 119SURFCOM 1400D-3DF apparatus.

Corrosion behaviour was investigated by potentiodynamic polarization, with a Bio-logic SP-50 equipment, in 0.1 M NaCl and 0,1 M NaOH solution. The system was a standard three-electrode cell, with a platinum plate counter electrode and Ag/AgCl (KCl saturated) reference
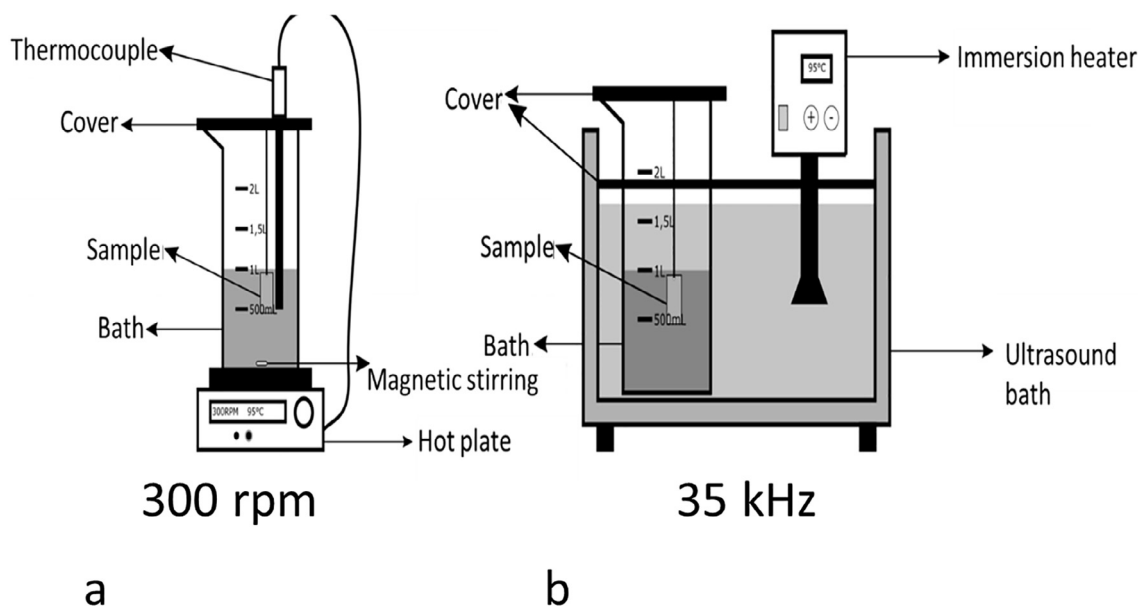

Fig. 1. Agitation systems used for electroless nickel-boron plating. a) Mechanical agitation – b) ultrasonic agitation.
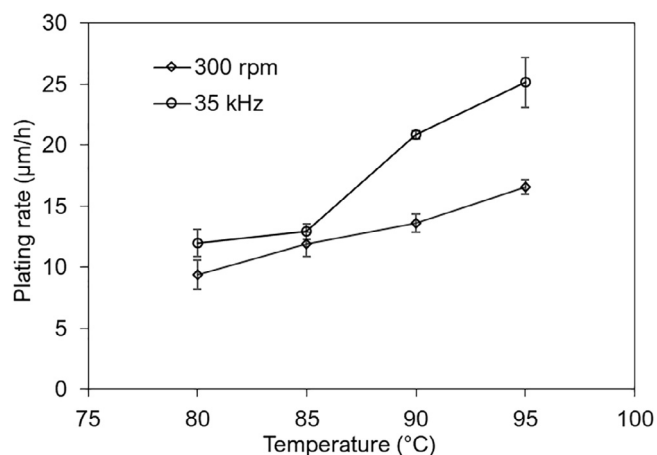
Fig. 3. Evolution of the plating rate of electroless nickel-boron with temperature and agitation method.

electrode. A settling time of 20 min at OCP was respected before the polarization experiment and the potential range was ± 0.6 V Vs OCP, with a 1 mV/s scan rate.

Tribological behaviour was measured with a pin-on-disc CSM microtribometer, in non-lubricated conditions, with the coated samples as discs and 6 mm alumina ball (hardness = 1400 HV) as the pin. The testing conditions were 10 cm/s, for a total length of 100 m, a normal load of 5 N. The temperature was 20 °C and relative humidity was 45%.

Tribocorrosion tests were carried out in a modified pin-on-disc tribometer (the one presented before), with the following conditions: normal load of 5 N, speed 5 cm/s, total length 100 m, corrosive solution: NaCl 0.1. Counterpart: alumina ball (6 mm). The load and speed were reduced for this test to avoid liquid projection during the experiment: in this system, presented on Fig. 2, the sample is placed in a cup-shaped water-tight holder that rotates while the pin is stationary.

3. Results and discussion

3.1. Deposition rate, morphology and roughness

Plating rate was determined by measurement of coating thickness after 1 h of plating. It is presented in Fig. 3. Plating rate increases with temperature for both mechanical agitation and ultrasonic agitation. However, the increase is more marked for ultrasonic agitation in the 90–95 °C range and samples obtained with ultrasound assistance are always thicker than samples obtained with mechanical agitation at the same temperature. This is in complete accordance with the results of previous studies on ultrasound assistance in electroless plating [24,26,30,40]. The thickness obtained for a temperature of 80 °C is very low (less than 15 μm for both ultrasound and mechanical agitation). For this reason, only hardness and roughness of those samples will be investigated.

The surface morphology of coatings is presented in Figs. 4 and 5 (for SEM observation of ultrasound-assisted coatings). All coatings present a
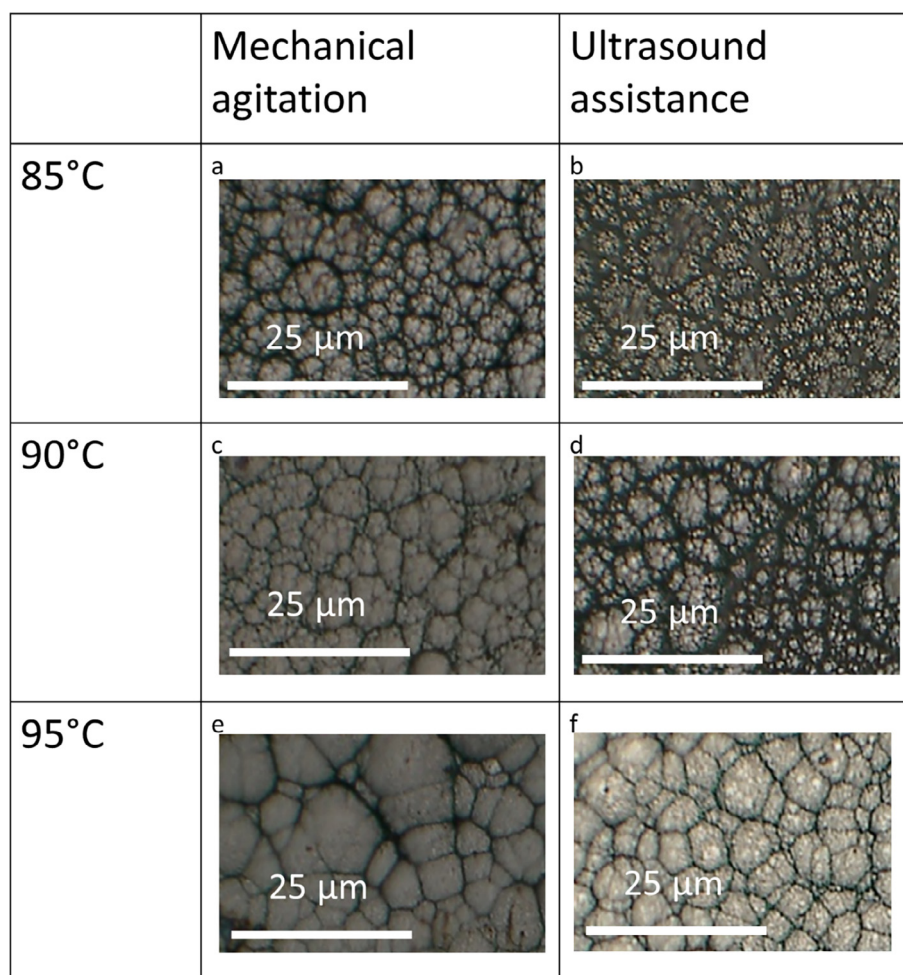

Fig. 4. Surface morphology of electroless nickel-boron coatings (optical microscopy). a- 85 °C, mechanical agitation; b- 85 °C, ultrasound agitation; c- 90 °C, mechanical agitation; d- 90 °C, ultrasound agitation; e- 95 °C, mechanical agitation; f- 95 °C, ultrasound agitation.
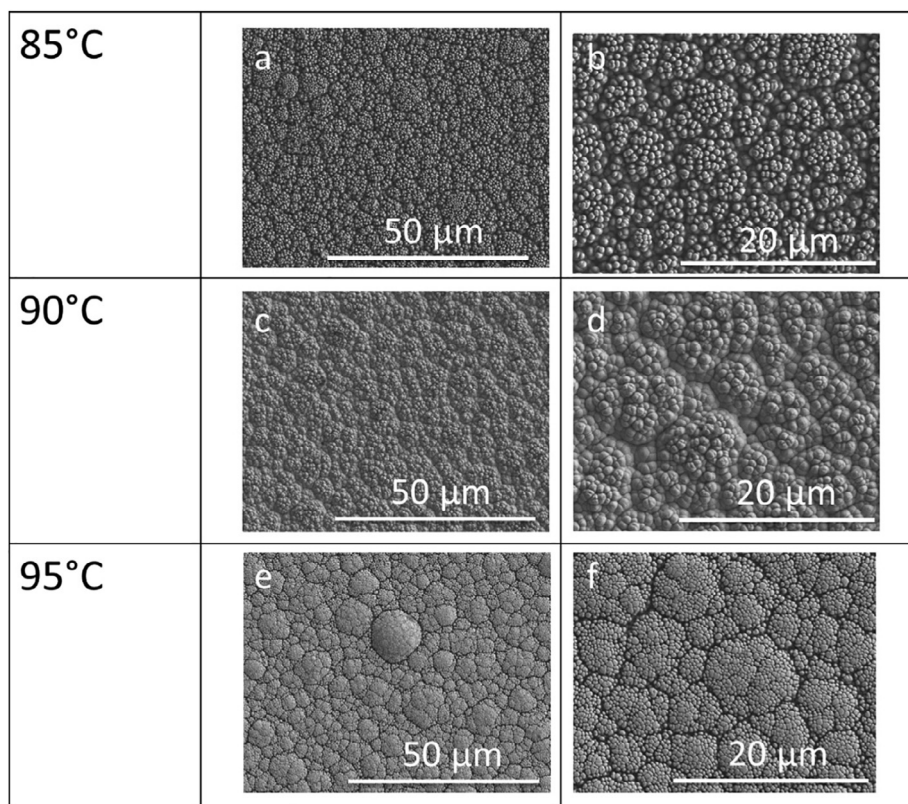
Fig. 5. Surface morphology of ultrasound-assisted electroless deposits (SEM). a, b: 85 °C; c-d: 90 °C; d-e: 95 °C.
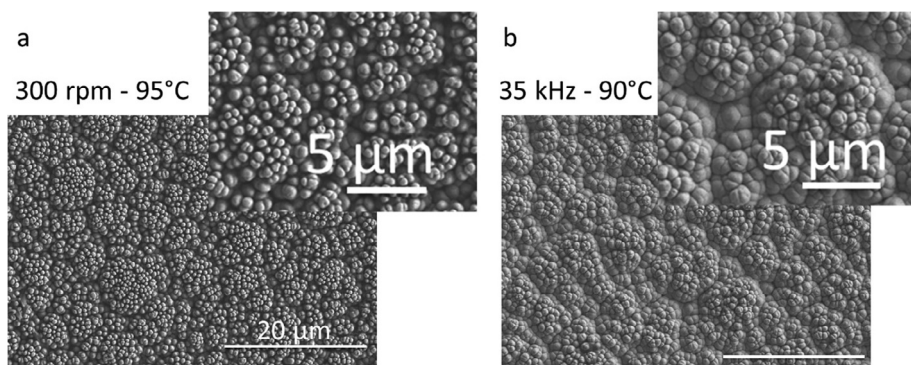

Fig. 6. Comparison of surface morphology (SEM) of a: coating obtained with mechanical agitation at 95 °C; b: coating obtained with ultrasound agitation at 90 °C.

cauliflower-like morphology, as is typically observed for electroless nickel-boron coatings synthesized with sodium borohydride as reducing agent and lead-based stabilizing agent [7,39]. However, the size of the features (nodules) increases with temperature and is systematically smaller in the case of ultrasound-assisted deposition than for mechanical agitation. The morphology of a coating obtained with ultrasound at 90 °C is the same as that of one used with mechanical agitation at 95 °C as attested by Fig. 6. The effect of temperature on the thickness and size of features is explained by kinetics: at a higher temperature, the transport of reactive species to the active surface sites is increased, leading to quicker deposition but has no effect on nucleation. The size of features increases thus with increasing temperature. Ultrasound agitation also enhances transport phenomena, leading likewise to an increase in plating rate. However, the cavitation phenomena occurring at the surface of the growing coating lead to an increase of surface activity, by degassing of adsorbed hydrogen among other phenomena. This increased activity leads in turn to a higher nucleation rate for new aggregates and thus to smaller features than in the case of mechanical

agitation. This effect is a well-known effect of ultrasound assistance [29,33].

The increase of the difference in plating rate between mechanical agitation and ultrasound with increasing temperature is due to the fact that, while increasing temperature increases the transport phenomena of species, it has no effect, as explained before, on the formation of the coating. The use of ultrasound enables thus species that are transported quicker to the surface to be more easily deposited.

Cross section observation of the coatings (Fig. 7) shows that all coatings present a columnar morphology, as expected from the plating bath composition. This observation also confirms that, while ultrasound generates thicker coatings, the columns present in those coatings are thinner than in the case of mechanical agitation, leading to finer surface features. The refinement of columns with increasing temperature is also observed on cross-section.

Roughness measurements (Fig. 8) confirmed the refinement of columns and superficial features with increasing temperature: roughness decreases from 1.05 μm to 0.25 μm and from 0.8 μm to 0.2 μm for
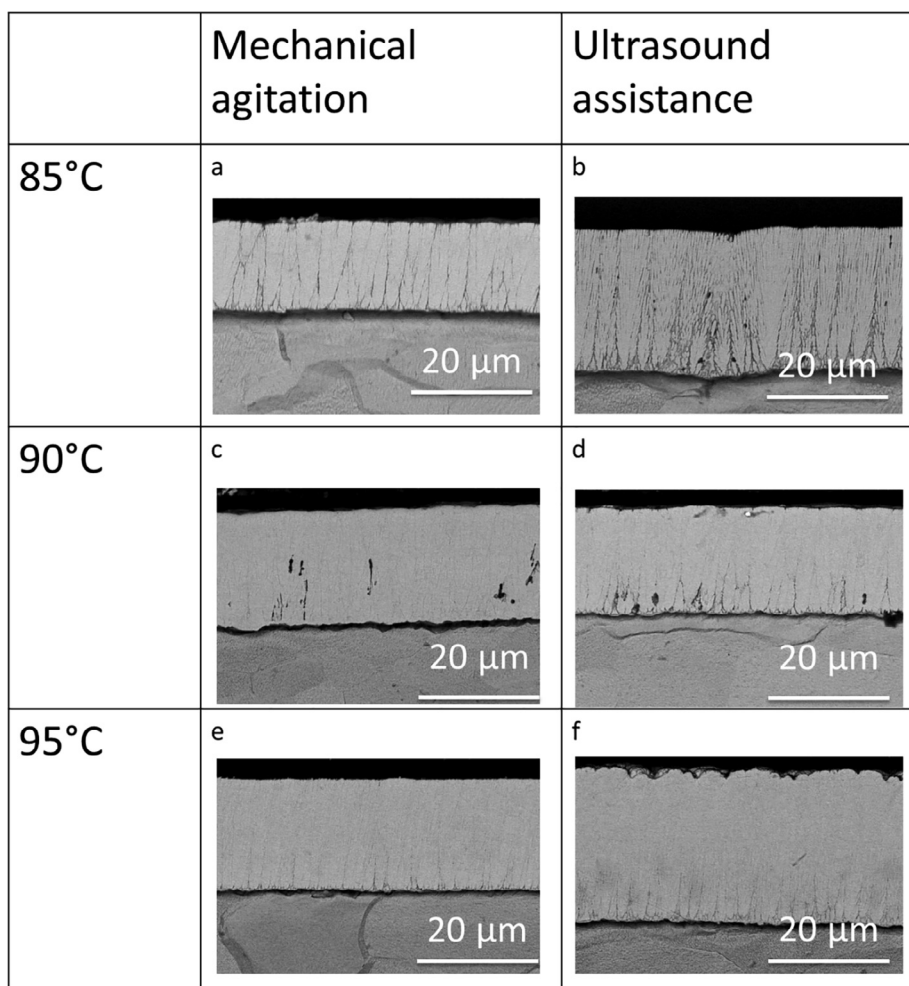
Fig. 7. Cross-section morphology of electroless nickel-boron coatings (SEM). a- 85 °C, mechanical agitation; b- 85 °C, ultrasound agitation; c- 90 °C, mechanical agitation; d- 90 °C, ultrasound agitation; e- 95 °C, mechanical agitation; f- 95 °C, ultrasound agitation.
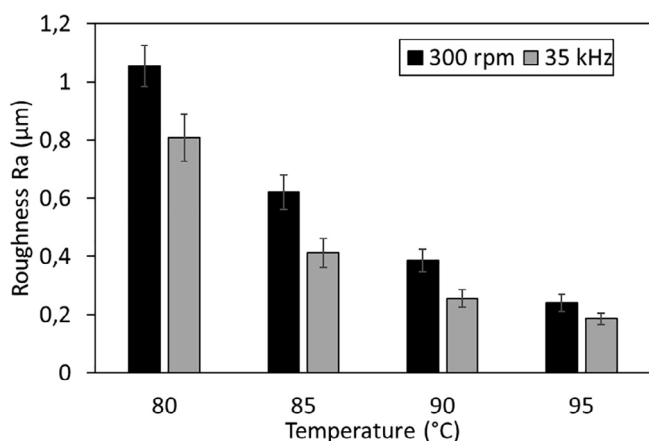

Fig. 8. Evolution of roughness of electroless nickel-boron coatings with temperature and agitation method.

mechanical ultrasound agitation, respectively, when temperature increases from 80 to 95 °C. Ultrasound-assisted samples present lower roughness compared to mechanical agitation for all temperatures and the similarity of properties between samples obtained at 95 °C with mechanical agitation and at 90 °C with ultrasound assistance is confirmed: both types of samples present a roughness of 0.25 μm.

3.2. Hardness and wear behaviour

The hardness of the electroless nickel-boron coatings is presented in Fig. 9. The evolution of hardness with temperature presents very different behaviour for samples obtained with mechanical agitation and with ultrasound agitation. The first present a significant increase with temperature, from approximately 500 hk_{50} at 80 °C to more than 800 k_{50} at 95 °C. This increase cannot be attributed to variations in thickness because the measurements were carried out on cross-section to avoid this problem. This increase of hardness is linked to differences in the formation of the coating that are attested by the difference in morphology shown in Fig. 7. At higher temperature, the coating appears denser and more closely packed, which allows reaching optimal hardness.

In the case of coatings obtained with ultrasound assistance, that present in all cases a significantly finer microstructure than coatings from mechanically agitated baths, except for high temperatures (95 °C), the hardness of the coating is always close to 800 hk_{50} and no significant increase is observed. This is probably due to the fact that ultrasound assistance leads to morphological refinement. This refinement allows coatings to reach the optimal hardness or be close to it) even for significantly lower temperature.

Tribological characterization was carried out on ultrasound-assisted coatings as well as on the standard coating (95 °C, mechanical agitation). Ultrasound assistance increases significantly the wear resistance of coatings, as can be seen in Table 2, with values of specific wear rate, nearly halved compared to the standard coating, without any effect of
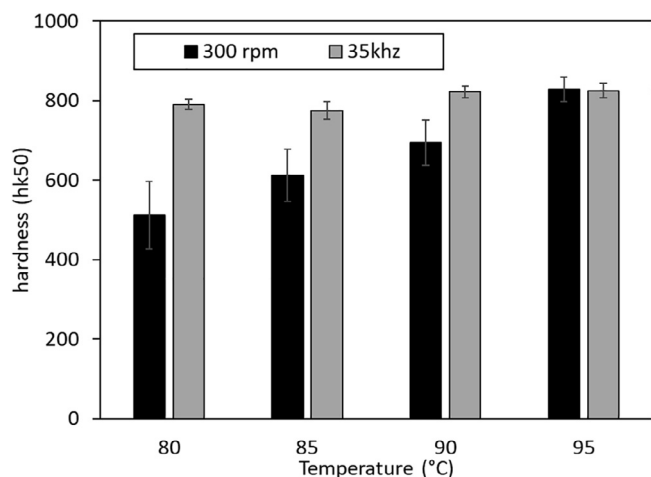
Fig. 9. Evolution of hardness of electroless nickel-boron coatings with temperature and agitation method.

Table 2
Tribological properties of electroless nickel-boron coatings.

	Specific wear rate (μm^2/N)	Friction coefficient (after 100 m)	Wear track width (μm)
NiB 95 °C 300 rpm	0.28	0.61	186
NiB 85 °C 35 kHz	0.14	0.38	150
NiB 90 °C 35 kHz	0.18	0.23	161
NiB 95 °C 35 kHz	0.13	0.43	146

the plating temperature. These results are in concordance with the hardness values of the coatings: all the samples obtained by ultrasound-assisted electroless plating present hardness values comparable to that of the standard samples (95 °C, mechanical agitation).

The friction coefficient measured after 100 m of pin-on-disc testing is also significantly lower for coatings obtained with ultrasound assistance, but in this case, temperature appears to have more influence: the

coating obtained at 90 °C presents the lowest friction coefficient, with a value of 0.23. The width of wear tracks follows an opposite trend, with wider tracks for the samples presenting the lower friction coefficient, which suggest that slightly different wear mechanisms occur for samples obtained at various temperatures.

Observation of the wear tracks (Fig. 10) showed, as expected, much lighter damage on the coatings prepared with ultrasound agitation, whatever the temperature, than on the standard coating. Coatings obtained with mechanical agitation (Fig. 10a) presented deep grooves similar to abrasive wear damage and the cauliflower-like surface texture has been nearly completely worn away in the track zone. In the case of coatings obtained with ultrasound agitation, the cauliflower-like texture can still be observed in the damaged zone. Wear grooves are clearly observable for the coating synthesized at 85 °C (Fig. 10b) and, to a lesser extent on the one made at 95 °C (Fig. 10d) but they are not observed on the coating deposited at 90 °C (Fig. 10c), where the only damage is flattening of the higher part of the columns and can be assimilated to burnishing.

Observation of the wear counterparts (alumina balls) have shown that there were only negligible variations between coatings in this study and that the wear mechanism is a combination of adhesive and abrasive wear, but the quantity of matter transferred from the coating to the counterpart was limited, as already said in a previous paper for coatings synthesized at 95 °C [37]. The main wear mechanism is thus abrasion.

3.3. Corrosion and tribocorrosion behaviour

Corrosion of the samples was investigated in neutral (0.1 M NaCl) and alkaline (0.1 NaOH) media. Acidic media were voluntarily not selected at this stage of the study because the standard nickel-boron coating does not present strong corrosion resistance in that environment [41,42].

In NaCl 0.1 M (Fig. 11a), the polarization curve of ultrasound-assisted electroless nickel-boron coatings shifts towards more negative potential when the temperature increases. This suggests that increasing the plating temperature will be detrimental to the corrosion resistance of the coatings. This may be linked to some extent to the refinement of
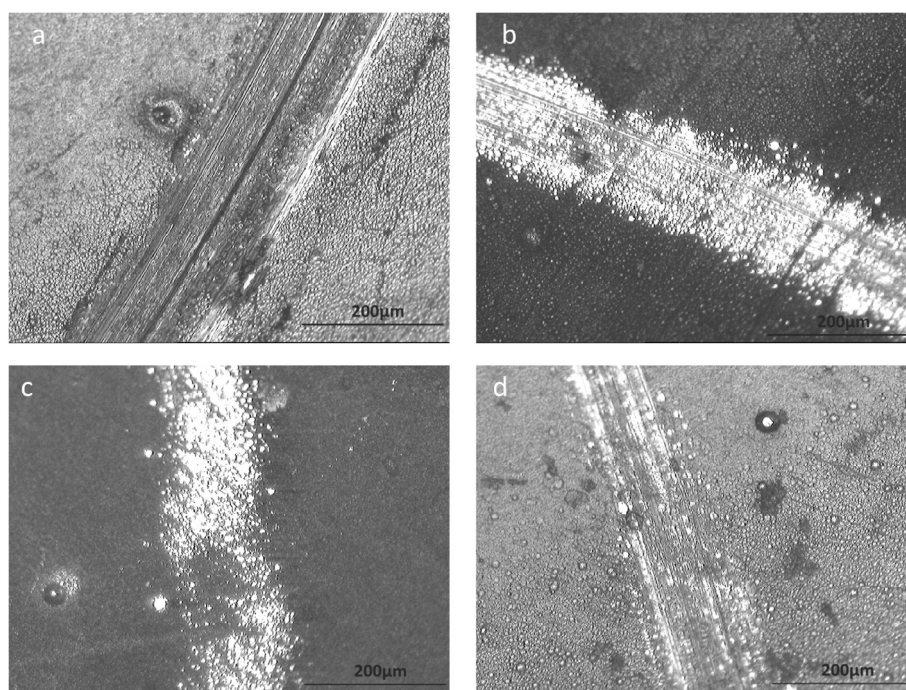

Fig. 10. Wear tracks on electroless nickel-boron coatings: a- 95 °C, mechanical agitation; b- 85 °C, ultrasound agitation; c- 90 °C, ultrasound agitation; d- 95 °C, ultrasound agitation.
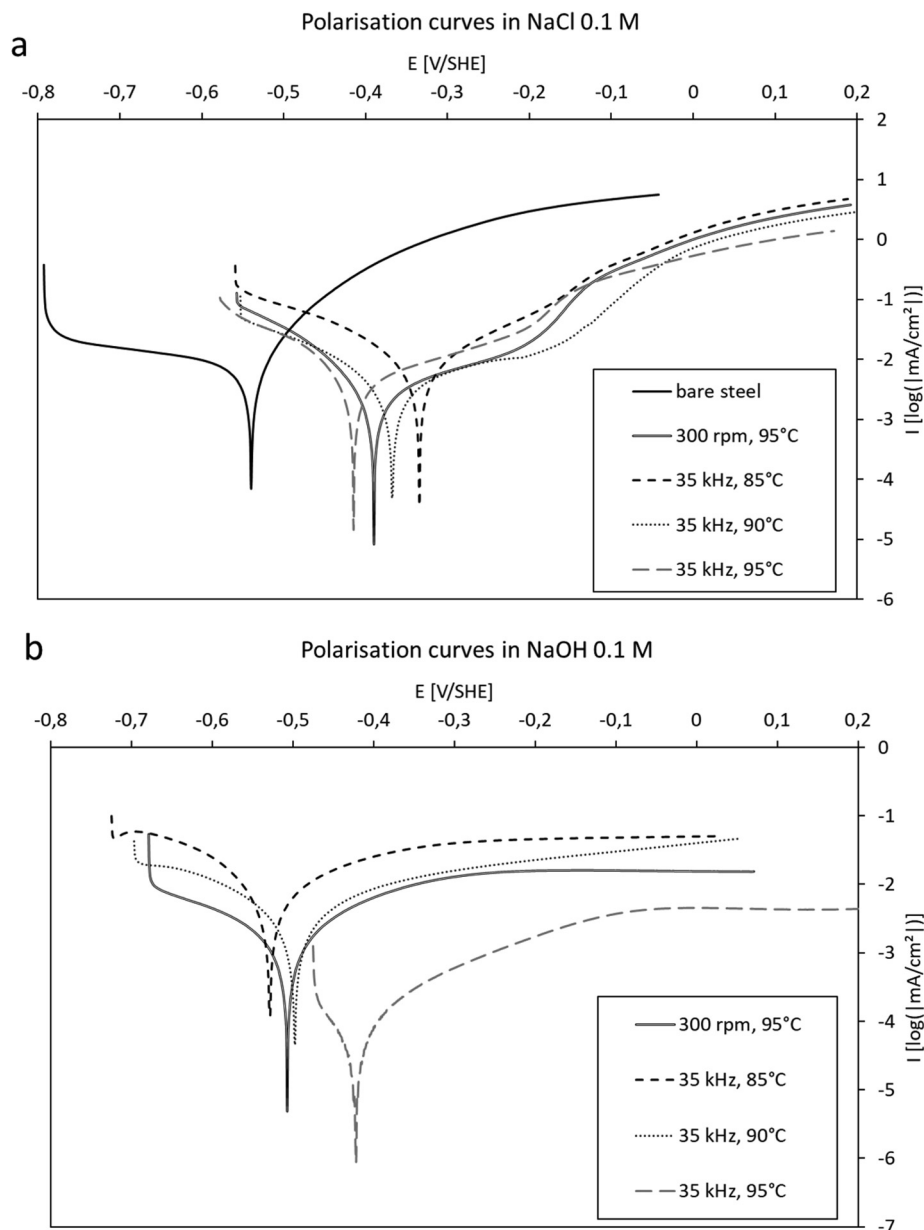
Fig. 11. Potentiodynamic polarization curves on electroless nickel-boron samples in a- 0.1 M NaCl; b- 0.1 M NaOH.

Table 3
Specific wear rate in tribocorrosion conditions.

	NiB 95 °C 300 rpm	NiB 85 °C 35 kHz	NiB 90 °C 35 kHz	NiB 95 °C 35 kHz
Specific wear rate (μm^2/N) in standard wear conditions	0.28	0.14	0.18	0.13
Specific wear rate (μm^2/N) in tribocorrosion conditions	0.30	0.39	0.16	0.37

coating morphology: finer columns are accompanied by a greater number of intercolumnar spaces, that are potential corrosion paths. It has been indeed proved that the main corrosion damage occurring in electroless nickel-boron coatings in sodium chloride is intercolumnar corrosion [43]. The coatings obtained at 90 °C with ultrasound agitation presents, once again, the closest behaviour to the standard coating (obtained at 95 °C with mechanical agitation), the only difference being a slight shift towards more positive potential. The shape of the polarization curve is even similar for those two coatings, suggesting similar corrosion behaviour. None of the coatings presents passive behaviour in NaCl.

In sodium hydroxide (Fig. 11b), all the coatings present a strong passive behaviour in alkaline solution, as expected for electroless nickel-boron. In this case, the influence of temperature is more marked, with a decrease of corrosion current, including in the passivation zone and a shift towards less negative corrosion potential when plating temperature increases. The coatings obtained with ultrasound assistance at 95 °C presents the best results in this case, with a very significant potential shift compared to other coatings. It is interesting to note that the coating obtained at 90 °C with ultrasound presents a polarization curve very similar to the standard coating obtained with mechanical agitation.
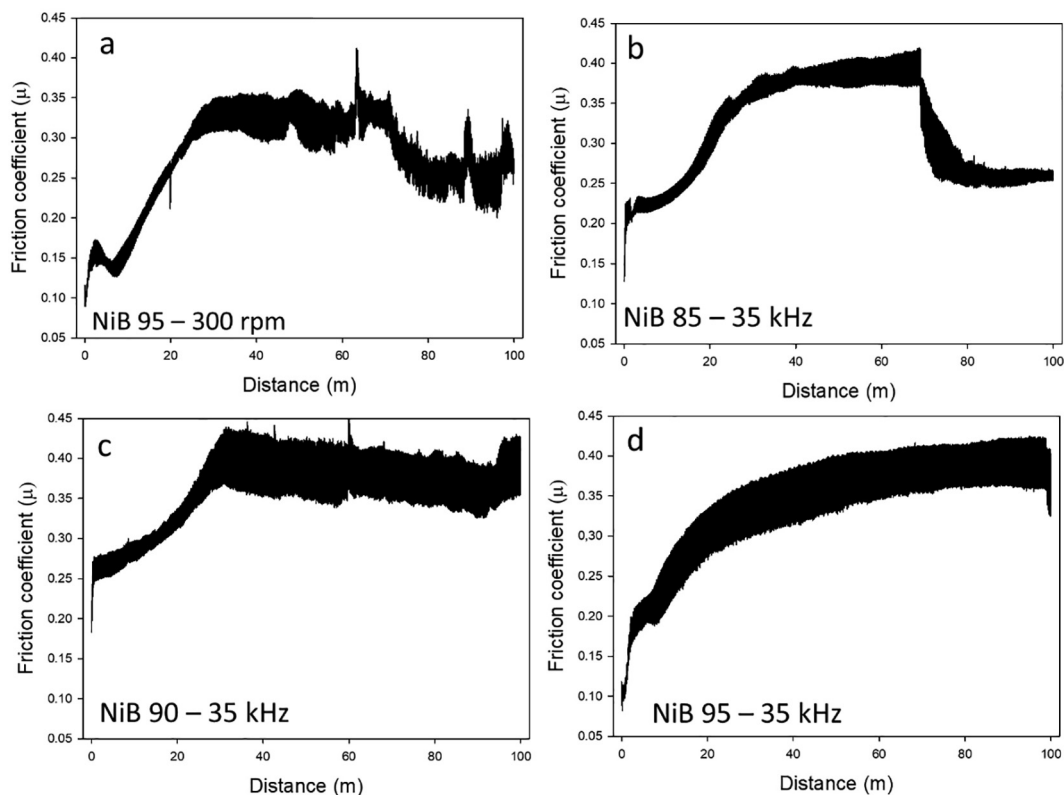
Fig. 12. Evolution of friction coefficient during pin-on-disc tribocorrosion test in 0.1 M NaCl: a- 95 °C, mechanical agitation; b- 85 °C, ultrasound agitation; c- 90 °C, ultrasound agitation; d- 95 °C, ultrasound agitation.

Fig. 13. Wear tracks on electroless nickel-boron coatings after pin-on-disc tribocorrosion test in 0.1 M NaCl: a- 95 °C, mechanical agitation; b- 85 °C, ultrasound agitation; c- 90 °C, ultrasound agitation; d- 95 °C, ultrasound agitation.
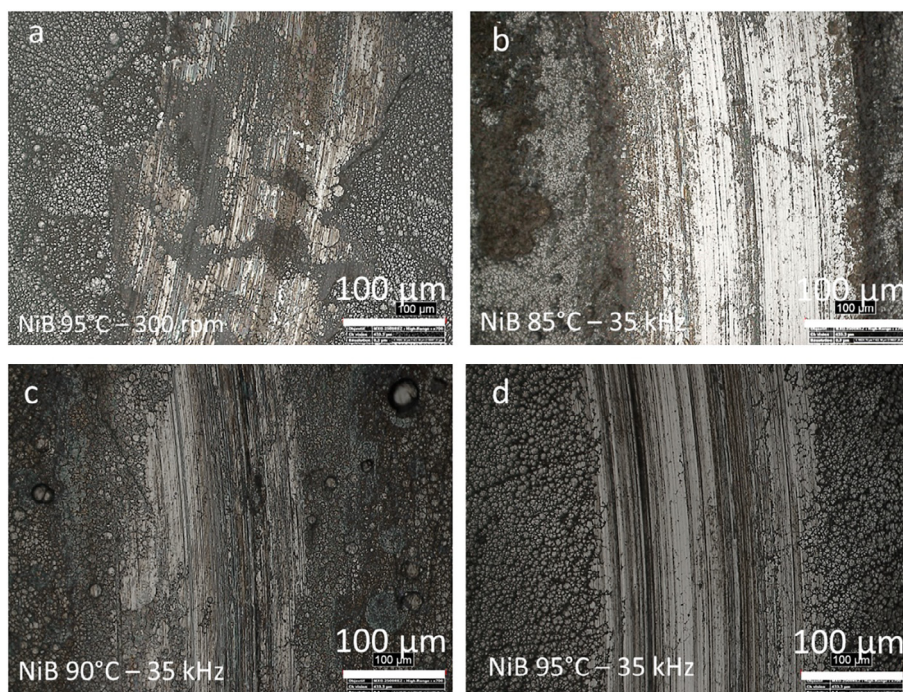
The results of potentiodynamic polarization suggest that the use of ultrasound would not damage corrosion resistance of electroless nickel-boron coatings and could even improve it in some conditions. This has to be validated by salt-spray tests in future work.

Tribocorrosion tests, in neutral chloride medium, did have different effects on different samples. As shown in Table 3, the standard samples obtained with mechanical agitation and the samples synthesized with ultrasound assistance at 90 °C presented very similar specific wear rates in NaCl medium and in air. However, the specific wear rate of the other samples obtained with ultrasounds, that presented better results in air,
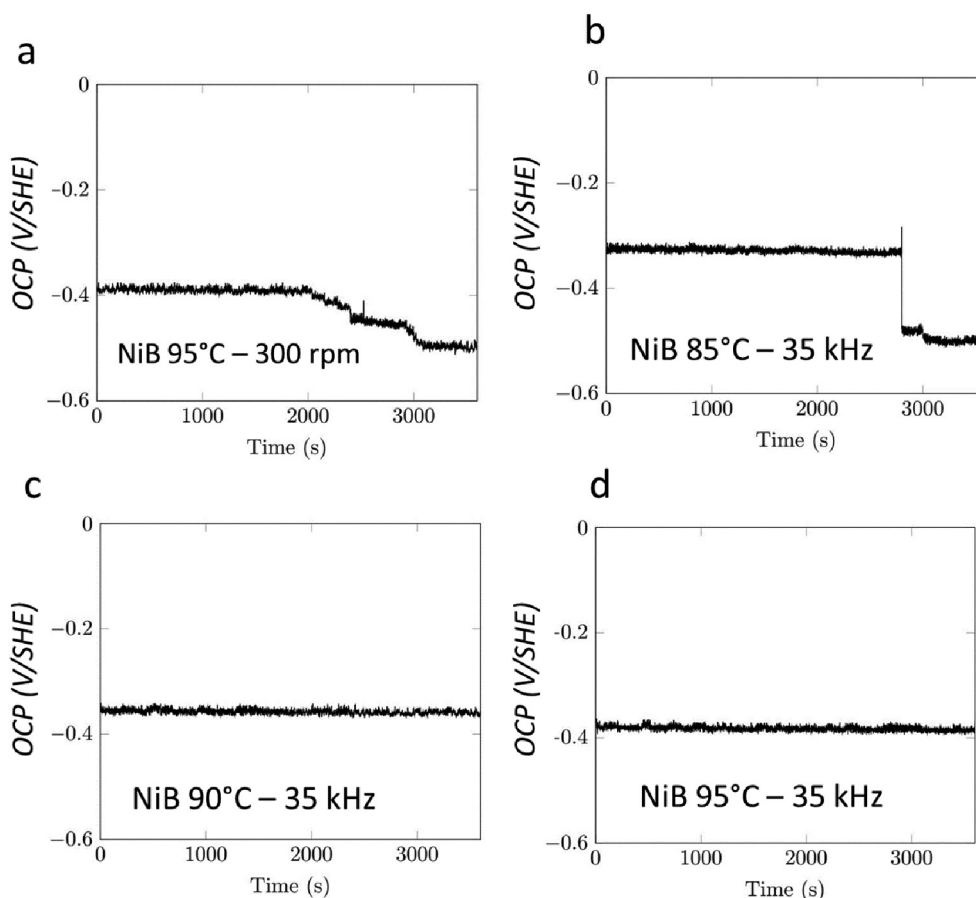
Fig. 14. Evolution of OCP during pin-on-disc tribocorrosion test in 0.1 M NaCl: a- 95 °C, mechanical agitation; b- 85 °C, ultrasound agitation; c- 90 °C, ultrasound agitation; d- 95 °C, ultrasound agitation.

were much higher in saline solution and reached specific wear level similar to (and even slightly higher than) the standard sample, that showed initially the worst behaviour.

To understand this, the evolution of the friction coefficient with testing distance was studied in details (Fig. 12). The samples that were not affected by the change of testing medium (standard sample and ultrasound assisted sample obtained at 90 °C) presented similar evolutions of the coefficient of friction: a break-in period during the first 30 m during which the friction coefficient increased, followed by a slow decrease of friction coefficient. In the case of the standard coating, significant variations were observed during this second period but the decrease was very smooth for the samples synthesized at 90 °C with ultrasound agitation, which probably explains the better specific wear rate. The friction coefficient for the ultrasound assisted, 90 °C samples, was always slightly higher than that of the standard sample (in the 0.35–0.40 range and lower than 0.35 respectively).

The other two samples presented completely different evolutions of friction coefficient: A break-in period followed by a plateau at 0.4, then a sharp decrease and a stabilization around 0.95 for the sample synthesized at 85 °C with ultrasound and an slow increase with asymptotical behaviour at 0.4 for the one synthesized with ultrasound at 95 °C.

Those behaviours and variations can be partially explained by microscopy observation of the worn zone (Fig. 13): samples synthesized with ultrasound at 85 and 95 °C present deep wear grooves and the surface texture is completely worn off in the wear area. The other two samples present less prominent grooves and the surface texture can still be observed in the wear area.

Another element of explanation can be obtained from the evolution of the open circuit potential (OCP) during the tribocorrosion test (Fig. 14). The samples synthesized with ultrasound at 85 °C, which

presents a sharp variation of friction coefficient during the test and deep wear grooves also presents a sudden drop in OCP. This is most probably linked with complete wear of the coating per places (this sample is thinner than the others and presents also slightly lower hardness and coarser features), exposing the substrate (the drop in OCP corresponds to the difference in corrosion potential between the substrate and nickel, as shown in Fig. 11).

The sample synthesized without ultrasound also presents a decrease of OCP with time, that comes in several steps, which corresponds to variations in the friction coefficient curve. Those may correspond to the presence of zones where the coating is completely worn out, but the observation of the worn surface does not really confirm that.

The samples synthesized at 95 °C with ultrasound assistance does not present a shift in OCP during tribocorrosion test (Fig. 14d) but it has a high specific wear rate. The reason for the absence of shift is most probably linked with the fact that this sample is thicker. There is thus remaining coating on every point of the surface, even with wear damage similar to the previous two samples.

Finally, the samples synthesized at 90 °C with ultrasound assistance, which presented a very low specific wear rate and a decreasing coefficient of friction after the break-in period also did not present a shift in OCP since there are no parts of the substrate where the coating is worn out.

4. Conclusions

The effect of temperature in the 80–95 °C range and of ultrasound agitation on the properties of electroless nickel-boron was investigated in this study.

The plating rate increases with temperature, but this effect is more

marked when ultrasound agitation is used than in the case of mechanical agitation, leading to an increase of plating rate by more than 50% for a temperature of 95 °C.

The morphology of the coatings is influenced by temperature and by ultrasound agitation: the columnar features present in the coatings are refined by an increase of temperature and by the use of ultrasound. This is accompanied by a decrease in surface roughness.

The hardness of the coatings increases with increasing temperature when magnetic stirring is used. In the case of ultrasound, there is no obvious effect of hardness and all coatings present a hardness that is similar to that obtained at 95 °C with mechanical agitation.

Wear behaviour in dry conditions of samples synthesized with ultrasound agitation is in all cases better than that of samples made at 95 °C with magnetic stirring, but this is not the case for tribocorrosion in 0.1 M NaCl: only the sample synthesized with ultrasound at 90 °C kept its good wear behaviour in those conditions and other samples performed similarly or worse than the sample made at 95 °C with mechanical agitation.

In NaCl medium, the highest corrosion potential was observed for the coating synthesized with ultrasound at the lowest temperature and the worst behaviours were observed for the two samples synthesized at 95 °C, with a slight advantage for the one made without ultrasound. However, in NaOH, all samples presented passive behaviour and the samples synthesized at higher temperatures presented the best behaviour, while the use of ultrasound also shifted the corrosion potential towards higher values.

The samples synthesized at 95 °C under mechanical agitation and at 90 °C with ultrasound assistance presented similar behaviour in terms of morphology, roughness, hardness and corrosion resistance. However, the sample made with ultrasound agitation was thicker due to the increase of plating rate and presented a better wear behaviour in both dry and lubricated conditions. It constitutes a very good candidate for the replacement of the standard sample (synthesized in a plating bath at 95 °C under mechanical applications) in applications where wear is the most important solicitation and on substrates that don't tolerate high temperature (like polymers).

In future work, further characterization of the coatings synthesized with ultrasound assistance at 90 °C will be carried out to investigate abrasive wear and scratch test behaviour of those coatings, as well as their ability to be heat treated.

Acknowledgements

Appendix A. Supplementary data

Supplementary data to this article can be found online at https://doi.org/10.1016/j.ultsonch.2019.04.027.

References

[1] A. Brenner, G.E. Riddell, J. Res. Natl. Bur. Stand. 1946 (37) (1934) 31.
[2] J. C. Warf, K. H. Schaltegger, Method of Coating Steel with Nickel-Boron, 1955, US patent 2726170.
[3] V. Vitry, F. Delaunois, in Compr. Guid. Nanocoatings Technol. Vol. 1 Depos. Mech. (Ed.: M. Aliofkhazraei), Nova Science Publishers, 2015, pp. 145–173.
[4] J. Sudagar, J. Lian, W. Sha, J. Alloys Compd. 571 (2013) 183–204.
[5] R.A. Shakoor, R. Kahraman, W. Gao, Y. Wang, Int. J. Electrochem. Sci. 11 (2016) 2486–2512.
[6] P. Sahoo, S.K. Das, Mater. Des. 32 (2011) 1760–1775.
[7] V. Vitry, A. Sens, F. Delaunois, Mater. Sci. Forum 783–786 (2014) 1405–1413.
[8] L. Bonin, V. Vitry, Surf. Coatings Technol. 307 (2016) 957–962.
[9] V. Vitry, L. Bonin, Electrochim. Acta 243 (2017) 7–17.
[10] B. Luiza, V. Véronique, D. Fabienne, Mater. Manuf. Process. n.d., 33, DOI 10.1080/10426914.2017.1291949.
[11] V. Vitry, A.-F.F. Kanta, F. Delaunois, Mater, Sci. Eng. B Solid-State Mater. Adv. Technol. 175 (2010) 266–273.
[12] F. Jia, Z. Wang, Acta Phys.-Chim. Sin. 27 (3) (2011) 633–640.
[13] V. Vitry, A.-F.F. Kanta, F. Delaunois, Ind. Eng. Chem. Res. 51 (2012) 9227–9234.
[14] V. Vitry, A. Sens, A.-F. Kanta, F. Delaunois, in Met. 2012 - Conf. Proceedings, 21st Int. Conf. Metall. Mater., 2012.
[15] Haas Rohm, A. Solutions, Sodium Borohydride Digest (2003).
[16] J.P. Elder, A. Hickling, Trans. Faraday Soc. (1962) 1852–1864.
[17] L. Bonin, C.C. Castro, V. Vitry, A.-L. Hantson, F. Delaunois, J. Alloys Compd. 767 (2018) 276–284.
[18] I. Tudela, Y. Zhang, M. Pal, I. Kerr, A.J. Cobley, Surf. Coatings Technol. 259 (2014) 363–373.
[19] M.E. Hyde, R.G. Compton, J. Electroanal. Chem. 531 (2002) 19–24.
[20] I. Tudela, Y. Zhang, M. Pal, I. Kerr, T.J. Mason, A.J. Cobley, Surf. Coatings Technol. 264 (2015) 49–59.
[21] F. Su, C. Liu, P. Huang, Appl. Surf. Sci. 309 (2014) 200–208.
[22] M.K. Camargo, I. Tudela, U. Schmidt, A.J. Cobley, A. Bund, Electrochim. Acta 198 (2016) 287–295.
[23] P.B.S.N.V. Prasad, R. Vasudevan, S.K.K. Seshadri, S. Ahila, Mater. Lett. 17 (1993) 357–359.
[24] A.J. Cobley, T.J. Mason, V. Saez, Trans. Inst. Met. Finish. 89 (2011) 303–309.
[25] K. Kobayashi, A. Chiba, N. Minami, Ultrasonics 38 (2000) 676–681.
[26] A.J. Cobley, V. Saez, Circuit World 38 (2012) 12–15.
[27] V.K. Bulasara, R. Uppaluri, M.K. Purkait, Surf. Eng. 29 (2013) 489–494.
[28] A. Agarwal, M. Pujari, R. Uppaluri, A. Verma, Ultrason. Sonochem. 21 (2014) 1382–1391.
[29] J.E. Graves, M. Sugden, R.E. Litchfield, D.A. Hutt, T.J. Mason, A.J. Cobley, Ultrason. Sonochem. 29 (2016) 428–438.
[30] A.J. Cobley, B. Abbas, A. Hussain, Int. J. Electrochem. Sci. 9 (2014) 7795–7804.
[31] V.K. Bulasara, R. Uppaluri, M.K. Purkait, Mater. Manuf. Process. 27 (2012) 201–206.
[32] Y.S.S. Park, T.H.H. Kim, M.H.H. Lee, S.C.C. Kwon, Surf. Coat. Technol. 153 (2002) 245–251.
[33] F. Touyeras, J.Y. Hihn, S. Delalande, R. Viennet, M.L. Doche, Ultrason. Sonochem. 10 (2003) 363–368.
[34] J. Guo, Y. Hou, C. Yang, Y. Wang, L. Wang, Mater. Lett. 67 (2012) 151–153.
[35] J. Guo, Y. Hou, C. Yang, Y. Wang, H. He, W. Li, Catal. Commun. 16 (2011) 86–89.
[36] A. Chiba, H. Haijima, K. Kobayashi, Surf. Coat. Technol. 169–170 (2003) 104–107.
[37] L. Bonin, N. Bains, V. Vitry, A.J. Cobley, Ultrasonics 77 (2017) 61–68.
[38] V. Niksefat, M. Ghorbani, J. Alloys Compd. 633 (2015) 127–136.
[39] F. Delaunois, J.P. Petitjean, M. Jacob-Dulière, P. Liénard, Surf. Coat. Technol. 124 (2000) 201–209.
[40] W. Qian, H. Chen, C. Feng, L. Zhu, H. Wei, S. Han, G. Li, H. Lin, J. Jiang, Surf. Rev. Lett. 25 (2018) 1950006.
[41] L. Bonin, V. Vitry, F. Delaunois, Mater. Chem. Phys. 208 (2018) 77–84.
[42] F. Delaunois, V. Vitry, in Study Corros. Resist. Electroless Duplex NiP/NiB Coatings Differ. Media by Potentiodynamic Polarisation SEM Obs. Eurocorr 2014, 2014.
[43] A.F. Kanta, M. Poelman, V. Vitry, F. Delaunois, J. Alloys Compd. 505 (2010) 151–156.